

## Diffraction of dust acoustic waves by a circular cylinder

S.-H. Kim, J. R. Heinrich, and R. L. Merlino<sup>a)</sup>*Department of Physics and Astronomy, The University of Iowa, Iowa City, Iowa 52242, USA*

(Received 9 July 2008; accepted 14 August 2008; published online 23 September 2008)

The diffraction of dust acoustic (DA) waves around a long dielectric rod is observed using video imaging methods. The DA waves are spontaneously excited in a dusty plasma produced in a direct current glow discharge plasma. The rod acquires a negative charge that produces a coaxial dust void around it. The diameter of the void is the effective size of the “obstacle” encountered by the waves. The wavelength of the DA waves is approximately the size of the void. The observations are considered in relation to the classical problem of the diffraction of sound waves from a circular cylinder, a problem first analyzed by Lord Rayleigh [*Theory of Sound*, 2nd ed. (MacMillan, London, 1896)]. © 2008 American Institute of Physics. [DOI: [10.1063/1.2977986](https://doi.org/10.1063/1.2977986)]

Dust acoustic (DA) waves are pressure disturbances that propagate through the charged dust component in a dusty plasma.<sup>1–12</sup> They are very low-frequency waves, typically a few hertz to tens of hertz, since the wave inertia is carried by the heavy dust particles. DA waves are commonly observed in dusty plasmas formed in dc glow discharge plasmas where they are spontaneously excited, probably by an instability due to the ions drifting through the dust.<sup>13</sup> A novel aspect of DA waves is that they can be studied by video imaging of laser light scattered by the particles. The present investigation uses this technique to study the diffraction of dust acoustic waves by a dielectric obstacle. In this preliminary report, we present observations of DA wave diffraction by a long cylinder, which is essentially a two-dimensional geometry that is most amenable to laser light scattering and video imaging techniques.

The problem of the scattering (diffraction) of sound waves from a cylinder or a sphere was first considered by Lord Rayleigh in his classic treatise on sound.<sup>14</sup> The analysis of sound waves in a gas or DA waves in a dusty plasma leads to identical linearized continuity and momentum equations for small-amplitude perturbations,

$$\frac{\partial n}{\partial t} = -n_0 \nabla \cdot \vec{u}, \quad (1)$$

$$\frac{\partial \vec{u}}{\partial t} = -\frac{c_s^2}{n_0} \nabla n, \quad (2)$$

where  $n$  is the perturbed dust density,  $\vec{u}$  is the perturbed dust fluid velocity,  $n_0$  is the unperturbed dust density, and  $c_s$  is the propagation speed. We recognize Eqs. (1) and (2) as the Euler equations for an ideal (inviscid) compressible fluid. This similarity of the behavior of long-wavelength acoustic disturbances in a neutral gas and in an ionized gas<sup>15</sup> was pointed out explicitly by David Montgomery.<sup>16</sup> The form of the acoustic speed, of course, depends on the choice of the equation of state. For sound waves in a neutral gas,  $c_s = (\gamma k_B T / m)^{1/2}$  is the speed of sound, where  $\gamma$  is the ratio of specific heat at constant pressure to that at constant volume,

$T$  is the gas temperature,  $m$  is the mass of the gas molecules, and  $k_B$  is Boltzmann’s constant. For DA waves,  $c_s$  is the dust acoustic speed given by<sup>17</sup>

$$c_{\text{DA}} = \left( \frac{k_B T_d}{m_d} + \frac{\alpha Z_d^2 k_B T_i}{m_d [1 + (T_i/T_e)(1 - \alpha Z_d)]} \right)^{1/2}$$

where  $T_j$  ( $j=d, i, e$ ) is the (dust, ion, electron) temperature,  $\alpha = n_0/n_{i0}$  is the ratio of the unperturbed dust density,  $n_0$ , to the unperturbed ion density,  $n_{i0}$ , and  $m_d$  and  $Z_d$  are the dust mass and charge number, respectively.<sup>18</sup> The momentum equations for the neutral gas and dusty plasmas can be expressed in the similar form to Eq. (2) because the term containing the wave electric potential can be written in terms of the density perturbation,  $n$ , since for low-frequency DA waves, both electrons and ions can be considered to be in Boltzmann equilibrium.<sup>1</sup> For one-dimensional plane waves of the form  $\sim \exp[i(Kx - \omega t)]$ , where  $K$  and  $\omega$  are the wave number and angular frequency, respectively, the dispersion relation for the acoustic modes (gas or dust) is  $\omega = cK$ .

The experiments were carried out in a dc glow discharge device shown schematically in Fig. 1. A glow discharge was formed by applying 300–400 V to a 2.5 cm diameter anode disk located on the axis of a large (90 cm long by 75 cm diameter) grounded vacuum chamber that was backfilled with argon to a pressure  $\sim 100$  mtorr (13 Pa). The dc glow discharge was confined to a cylindrical region protruding roughly 15 cm from the anode by applying a uniform magnetic field up to  $\sim 0.01$  T along the axis of the vacuum chamber. Typical plasma parameters are  $n_e \sim 10^8 - 10^9 \text{ cm}^{-3}$ ,  $T_e \sim 2 - 3 \text{ eV}$ ,  $T_i \sim 0.03 \text{ eV}$ .<sup>7,12</sup>

The dusty plasma is produced using an electrically insulated tray loaded with kaolin powder (2 g/cc, nominal size 1  $\mu\text{m}$ ) and located below the anode. When the glow discharge is initially formed, dust particles are attracted into the plasma where they are confined under the opposing effects of electric forces and ion drag forces.<sup>7,10</sup> Assuming an average dust radius  $r_d \sim 0.5 \mu\text{m}$  (or  $m_d \sim 1 \times 10^{-15} \text{ kg}$ ), the dust charge number  $Z_d$ , estimated using the orbital motion limited (OML) model,<sup>19</sup> is  $Z_d \sim 1800$ . The dust particle cloud is illuminated with a 120 mW, diode pumped solid-state Nd:YAG laser operating at 532 nm, as shown in Fig. 1. The

<sup>a)</sup>Electronic mail: robert-merlino@uiowa.edu.

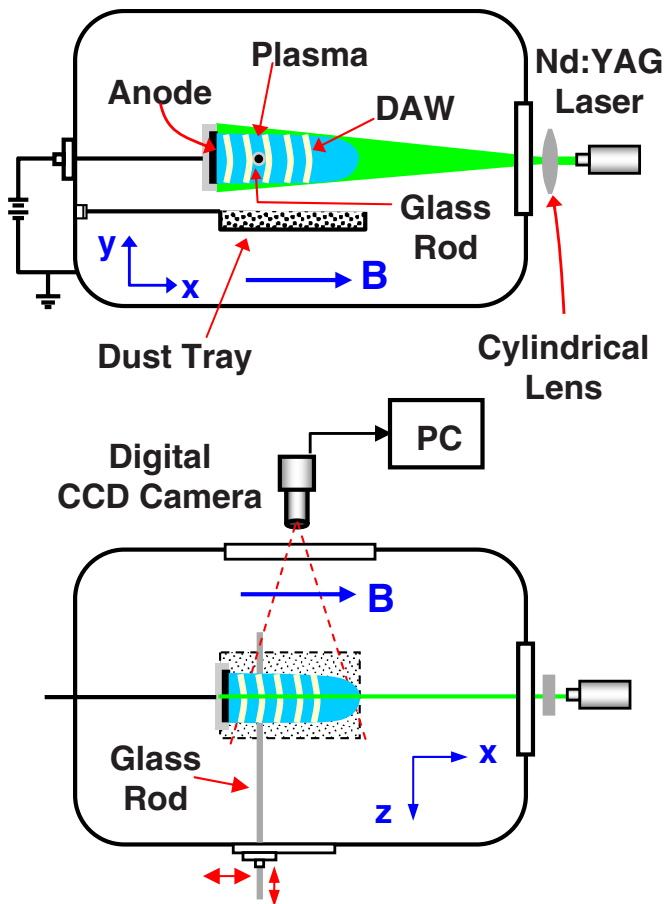


FIG. 1. (Color online) Schematic of the glow discharge dusty plasma device. The upper diagram is a side view showing the laser illumination geometry and the lower diagram is a top view showing the viewing geometry. The glow discharge is produced in argon at 100 mtorr (13 Pa) and 300 V. A longitudinal magnetic field up to 0.01 T is applied to form an elongated plasma fire-rod.

laser beam is expanded into a thin vertical sheet using a cylindrical lens and the scattered light is viewed and recorded using a digital charged-coupled device (CCD) camera fitted with a microscope lens and an optical filter that passes light at the laser wavelength. The CCD camera was operated at either 250 or 1000 frames/s. The output of the video camera was fed into a PC for processing. From the interparticle spacing measured from single frame video images, the average dust density is estimated to be  $n_0 \sim 10^{11} \text{ m}^{-3}$ .

Dust acoustic waves were spontaneously excited in the dusty plasma. The excitation of the DA waves is probably due to an instability driven by ions streaming through the dust.<sup>13</sup> The waves appeared as bright vertical fringes that propagated along the axis of the plasma away from the anode (the direction of ion flow). A single frame video image of the dust acoustic waves *before* the rod was inserted is shown in Fig. 2(a). The bright arcs are the compressional zones (condensations) of the waves that propagate, in this image, from left to right away from the anode disk, which is the bright rectangular structure on the left side of the image. From the single frame images, we estimate the wavelength of the DA waves to be  $\sim 2.5\text{--}3 \text{ mm}$ . It is also possible to follow the

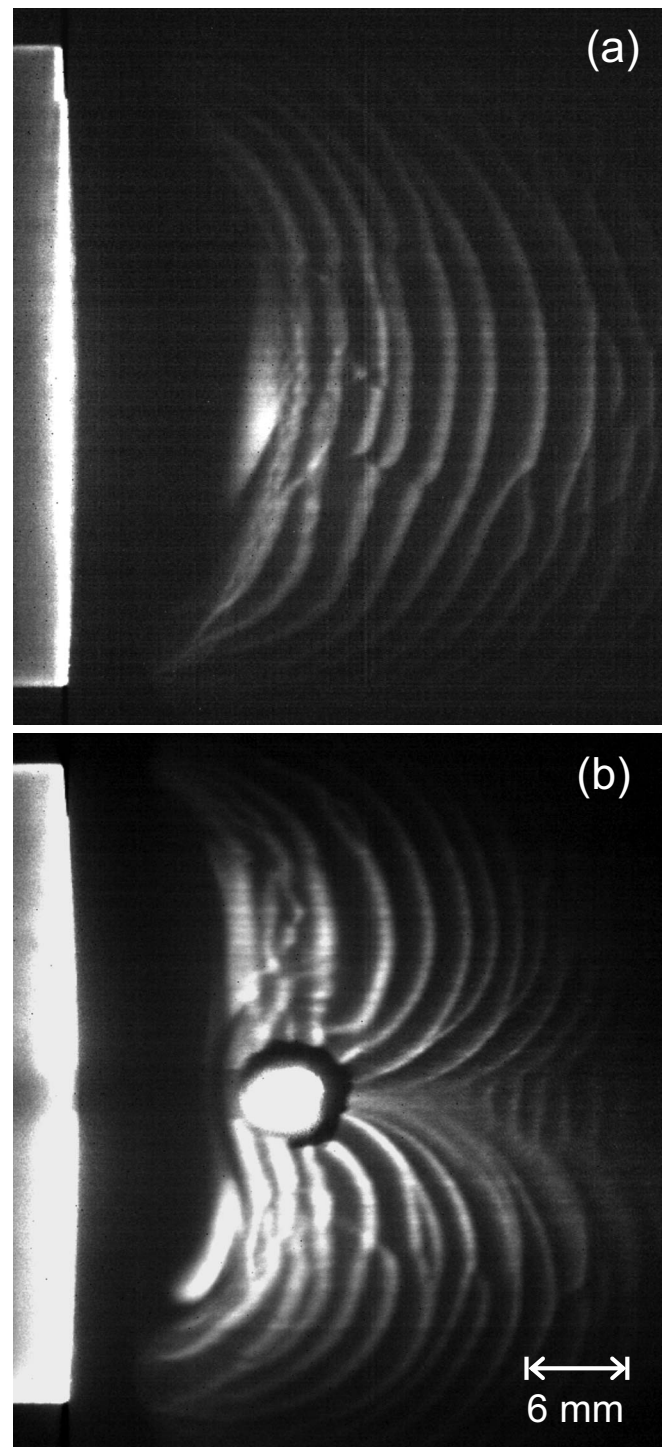


FIG. 2. Single frame video images of DA waves: (a) *Without* the rod present and (b) *with* the rod present. In both images, the anode is the white rectangle on the left. The bright circle in (b) is laser light captured in the rod and leaving the near end.

advance of the wavefronts in consecutive frames to obtain an estimate of the DA wave speed, which was  $\sim 25\text{--}30 \text{ cm/s}$ .

To study the interaction of the dust acoustic waves with a cylinder, a 3 mm diameter Pyrex tube was inserted into the dusty plasma, as shown in Fig. 1. A typical single frame video image of the DA wave interaction with the cylinder present is shown in Fig. 2(b). The size of the “obstacle” is determined not solely by its physical size but by the cylin-

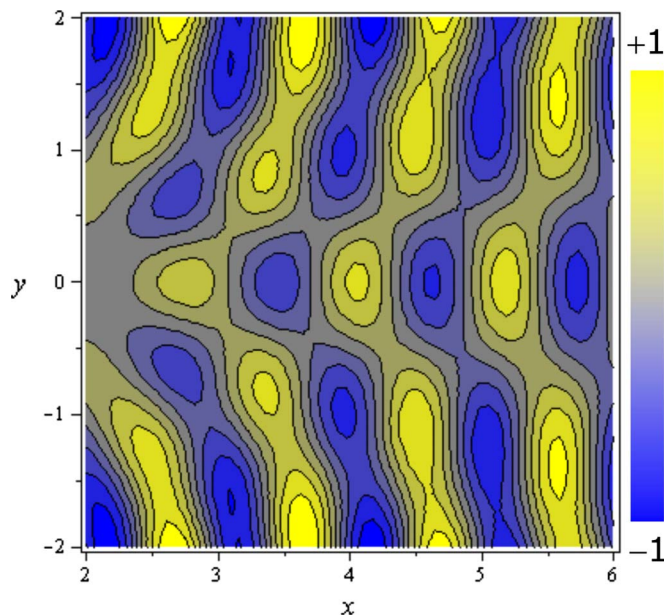


FIG. 3. (Color online) Two-dimensional contours of the acoustic pressure field downstream of a cylinder located at  $(0,0)$ . Here  $a=2$ ,  $\lambda=1$ , with all dimensions expressed in units of wavelength.

dical “void” (radius  $\sim 4$  mm) that surrounds the glass tube. The void forms due to the expulsion of the negatively charged dust particles by the inwardly directed electric field that develops around the rod because of the collection of electrons (with a thermal speed  $\gg$  the ion thermal speed) from the background plasma.<sup>20,21</sup> The diffraction of the DA waves around the rod is best appreciated by viewing a video sequence.<sup>22</sup> Upon encountering the obstacle, a DA wavefront splits into two vertical segments, each of which appears to attach to the circumference of the obstacle as they advance around it, until they merge near the equator on the downstream side and detach from the rod. The highly distorted wavefronts then continue to propagate downstream, with the central distorted section widening vertically and eventually flattening out far from the obstacle. At about 1 cm from the obstacle, secondary wavelets appear near the equatorial plane of the rod.

Since the DA waves and sound waves obey a similar set of equations, it is interesting to compare the resulting diffraction patterns in the two cases. The DA wave scattering problem occurs in the regime where the wavelength is comparable to the radius of the rod,  $\lambda \sim a$ , and neither the source nor the observation region are far from the object. This corresponds to the case of Fresnel diffraction in physical optics. In the analysis of the diffraction of sound, one usually considers two limiting cases that determine what boundary conditions are applied at the surface of the obstacle.<sup>23</sup> For an acoustically “hard” cylinder, the fluid velocity is taken to vanish on the surface, whereas for the acoustically “soft” cylinder, the pressure perturbation is taken to vanish. The acoustically soft cylinder condition is usually applied to scattering from a compressible object. It is not immediately clear which of these two conditions should apply, if either, to the present case. The dust particles comprising the fluid elements

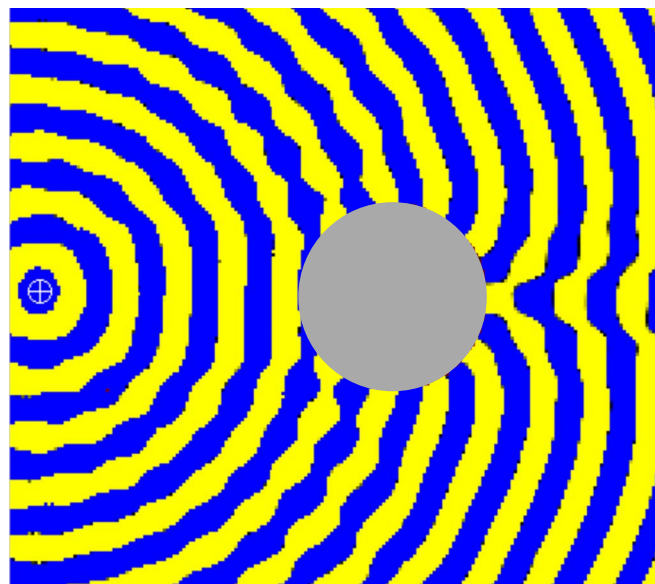


FIG. 4. (Color online) Image of a ripple tank simulation of waves from a point source interacting with a circular object.

that are the DA wave medium are excluded from the void region surrounding the negatively charged rod. Thus we will treat the void as a hard cylinder. An analytic solution of the scattering of plane sound waves from an infinite hard cylinder has been provided by Morse.<sup>24</sup> Briefly, the pressure in the sound wave is expressed as a sum of the undisturbed plane wave expanded in terms of cylindrical waves, and an outgoing cylindrical wave, with the condition that the radial fluid velocity of the combination vanishes at  $r=a$ . This leads to an infinite series for the pressure field  $p(r, \phi, t)$ , which can be evaluated for specified values of the parameter  $Ka=2\pi a/\lambda$ . Figure 3 shows the pressure field  $p(x, y)$  contours in a vertical plane for the case in which  $Ka=4\pi$  with all dimensions normalized to wavelengths. In the numerical evaluation of the pressure field, at least 20 terms were retained in the series to ensure convergence. The cylinder in Fig. 3 is located at  $(0,0)$  so that only the region downstream of the obstacle is shown. In comparing this result with that in Fig. 2, one needs to keep in mind that in the experiment, the incident waves are only approximately planar, whereas in Fig. 2 the incident sound waves are strictly planar. This accounts for the fact that in the DA case the pressure waves in the scattered field appear semicircular. Nevertheless, the acoustic simulation clearly shows the bending of the wavefronts as the wave passes by the cylinder followed by a gradual flattening-out as the waves progress downstream. The acoustic pressure resulting from the interaction of an acoustic Gaussian beam incident on a cylindrical object is given in Fig. 2 of Cummer and Schurig.<sup>25</sup>

A somewhat more realistic simulation of the diffraction of sound waves can be obtained using a ripple tank. It has been known for a long time that shallow water waves in a tank of about 1 cm depth provide an excellent model for sound in two dimensions.<sup>26</sup> A simulated ripple tank image of the diffraction of waves from a point source around a circular object is shown in Fig. 4.<sup>27</sup> The object is located several wave-

lengths downstream of the source to simulate roughly the curvature of the DA waves in the actual experiment.

In comparing the diffraction of the DA waves and ordinary sound waves, one should bear in mind that the DA waves are not launched from a localized source, as in the case of either the plane-wave source in Fig. 3 or the point source in Fig. 4. The DA waves are excited spontaneously in the dusty plasma as a result of an instability.

Finally, we point out that the diffraction of grid-launched *ion-acoustic* waves from an obstacle in a multidipole plasma was observed over 25 years ago by Okutsu, Nakamura, and Lonngren.<sup>28</sup>

This work was supported by DOE Grant No. DE-FG02-04ER54795.

We thank M. Miller for expert technical assistance. We are grateful to G. Morfill and V. Nosenko of the Max Planck Institute for Extraterrestrial Physics, Garching, Germany, for allowing us the use of the Photron video camera in this experiment. We also thank Paul Falstad for allowing us to display the output of the 2D wave applet.

<sup>1</sup>N. N. Rao, P. K. Shukla, and M. Y. Yu, *Planet. Space Sci.* **38**, 543 (1990).

<sup>2</sup>J. H. Chu, J.-B. Du, and L. I, *J. Phys. D* **27**, 296 (1994).

<sup>3</sup>N. D'Angelo, *J. Phys. D* **28**, 1009 (1995).

<sup>4</sup>A. Barkan, R. L. Merlino, and N. D'Angelo, *Phys. Plasmas* **2**, 3563 (1995).

<sup>5</sup>J. B. Pieper and J. Goree, *Phys. Rev. Lett.* **77**, 3137 (1996).

<sup>6</sup>H. R. Prabhakara and V. L. Tanna, *Phys. Plasmas* **3**, 3176 (1996).

<sup>7</sup>C. Thompson, A. Barkan, N. D'Angelo, and R. L. Merlino, *Phys. Plasmas* **4**, 2331 (1997).

<sup>8</sup>V. I. Molotkov, A. P. Nefedov, V. M. Torchinski, V. E. Fortov, and A. G. Khrapak, *JETP* **89**, 477 (1999).

<sup>9</sup>E. Thomas, Jr., *Phys. Plasmas* **13**, 042107 (2006).

<sup>10</sup>T. Trottenberg, D. Block, and A. Piel, *Phys. Plasmas* **13**, 042105 (2006).

<sup>11</sup>S. V. Annibaldi, A. V. Ivlev, U. Konopka, S. Ratynskaia, H. M. Thomas,

G. E. Morfill, A. M. Lipaev, V. I. Molotkov, O. F. Petrov, and V. E. Fortov, *New J. Phys.* **9**, 327 (2007).

<sup>12</sup>E. Thomas, Jr., R. Fisher, and R. L. Merlino, *Phys. Plasmas* **14**, 123701 (2007).

<sup>13</sup>M. Rosenberg, *J. Vac. Sci. Technol. A* **14**, 631 (1996).

<sup>14</sup>L. Rayleigh, *Theory of Sound*, 2nd ed. (MacMillan, London, 1896) (also Dover, New York, 1945).

<sup>15</sup>Langmuir referred to these plasma-ion oscillations as "electric sound waves." See I. Langmuir, *Proc. Natl. Acad. Sci. U.S.A.* **14**, 627 (1928).

<sup>16</sup>D. Montgomery, *Phys. Rev. Lett.* **19**, 1465 (1967).

<sup>17</sup>R. L. Merlino, A. Barkan, C. Thompson, and N. D'Angelo, *Phys. Plasmas* **5**, 1607 (1998).

<sup>18</sup>The effects of finite dust temperatures in dust plasmas in which  $T_d > T_e$  have recently been studied. See Ref. 12 and M. Rosenberg, E. Thomas, Jr., and R. L. Merlino, *Phys. Plasmas* **15**, 073701 (2008).

<sup>19</sup>H. Mott-Smith and I. Langmuir, *Phys. Rev.* **28**, 727 (1926).

<sup>20</sup>C. O. Thompson, N. D'Angelo, and R. L. Merlino, *Phys. Plasmas* **6**, 1421 (1999); E. Thomas, Jr., K. Avinash, and R. L. Merlino, *ibid.* **11**, 1770 (2004).

<sup>21</sup>The rod with the corresponding void is very similar to some 2D self-organized structures in confined dust systems observed in recent numerical simulations [Y. H. Liu, Z. Y. Chen, F. Huang, M. Y. Yu, L. Wang, and A. Bogaerts, *Phys. Plasmas* **13**, 052110 (2006); Y. H. Liu, Z. Y. Chen, M. Y. Yu, and A. Bogaerts, *Phys. Rev. E* **74**, 056401 (2006)], where a central cluster of dust grains replaces the rod.

<sup>22</sup>See EPAPS Document No. E-PHPAEN-15-038809 for two video clips of DA waves, one without the rod and one with the rod; both clips play at one frame per second. For more information on EPAPS, see <http://www.aip.org/pubservs/epaps.html>.

<sup>23</sup>R. T. Ling, *AIAA J.* **25**, 560 (1987).

<sup>24</sup>P. M. Morse, *Vibration and Sound* (McGraw Hill, New York, 1948), p. 347.

<sup>25</sup>S. Cummer and D. Schurig, *New J. Phys.* **9**, 45 (2007).

<sup>26</sup>A. H. Davis and G. W. C. Kaye, *The Acoustics of Buildings* (G. Bell and Sons, London, 1927); see also J. H. Rindel, *Revista de Acústica* **33**, 31 (2002), and J. Lighthill, *Waves in Fluids* (Cambridge University Press, Cambridge, 1978).

<sup>27</sup>There are many educational websites providing ripple tank simulations. Figure 4 was adapted from <http://www.falstad.com/mathphysics.html>.

<sup>28</sup>E. Okutsu, Y. Nakamura, and K. E. Lonngren, *J. Appl. Phys.* **53**, 861 (1982).